4

X-Ray Instrumentation

THE COMPONENTS of a typical energy-dispersive microanalysis system are shown schematically in Figure 4-1. It is the array of components from detector to multichannel analyzer that assembles the information contained in the x-ray signals into a convenient x-ray spectrum. The following paragraphs discuss these elements of the system, starting with the detector.

4.1 The Detector

All energy-dispersive spectrometers have in common a solid-state detector (Figure 4-2). For microanalysis, this detector is almost always manufactured from a single crystal of silicon. As with other semiconductors, the conductivity of silicon varies greatly, depending primarily on its purity and the perfection of its crystal lattice. In a perfect silicon crystal, there is a place for every electron and every electron is in its place. Impurities, however, disrupt this perfect structure, creating local abundances or shortages of electrons. The resulting free electrons or *holes* may serve as charge carriers under the influence of an

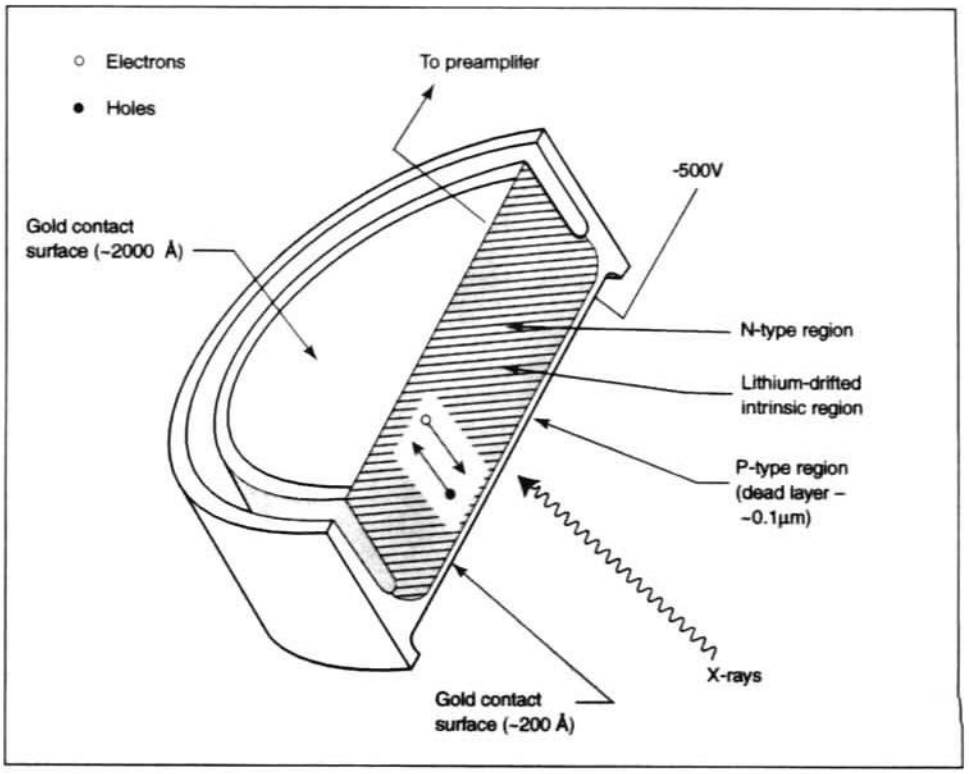

Figure 4-2. *Cross section of a typical lithium-drifted silicon detector. X-rays create electron-hole pairs in the intrinsic region of the semiconductor; these charge carriers then migrate to the electrodes under the influence of an applied bias voltage.*

applied electric field. Therefore, whereas a pure and perfect crystal conducts very little current, an imperfect one allows some current to pass. Ideally, a crystal of perfect structure and the highest purity is used for x-ray detection.

4.1.1 The Physics of X-Ray Detection

The silicon atoms making up the crystal are held in the periodic structure of the crystal by a covalent bonding mechanism that essentially shares electrons among the outer orbitals of several neighboring atoms. These shared electrons are said to occupy the *valence band* of the crystal. When an x-ray enters the crystal, there is a high probability that it will be absorbed in an interaction with an electron of one of the silicon atoms, producing a high-energy photoelectron. The ejected photoelectron eventually dissipates its energy in interactions that promote valence-band electrons to the *conduction band*, leaving holes in the once-filled valence-band.

Processes other than electron-hole pair generation (for example, heat generation) are involved in the dissipation of the energy deposited by the incoming x-ray. Nonetheless, a good statistical correlation exists between the amount of energy dissipated and the number of electron-hole pairs generated. On the average, 3.8 to 3.9 eV are dissipated in the creation of each electron-hole pair. This low value, relative to the energy of the x-ray (typically thousands of eVs), leads to the good statistical precision available from a silicon detector crystal.

The process of x-ray detection then becomes one of measuring the number of free charge carriers (electrons and holes) created in the crystal during the absorption of each x-ray. The crystal is operated as a reverse-bias diode under an applied voltage of 100 to 1000 volts. Any free charge created within the diode leads to a temporary increase in its conductivity. If the resulting current is integrated with respect to time, the total charge conducted is found to be directly proportional to the energy of the absorbed x-ray.

4.1.2 Leakage Current and Lithium Drifting

Even a perfect semiconductor crystal would be expected to show some residual conductivity upon which the momentary increases caused by x-ray absorption would be superimposed. Such baseline conductivity is due to the random thermal excitation of electrons across the gap between valence and conduction bands. To minimize this thermally induced background, or *leakage current*, detectors are operated at low temperatures. Most detectors therefore incorporate a liquid nitrogen cooling apparatus (or an electrically cooled apparatus) called a *cryostat*.

As we already mentioned, imperfections and impurities in the crystalline structure of the silicon also contribute to the conductivity of the crystal and therefore to the leakage current. In fact, silicon crystals pure enough to maintain the required bias voltage are not readily fabricated. Most contain impurities that cause excess holes to be present as *extrinsic* charge carriers. It is possible, however, to "compensate" for impurities and imperfections by a process known as *lithium drifting*. In this process, lithium atoms are allowed to diffuse into the crystal to compensate for the native impurities in the crystal. The result is a lithium-drifted silicon, or Si(Li), detector.

4.1.3 Spectral Resolution

Because of the complex nature of the interaction of the x-ray with the silicon crystal lattice and the competition among various energy-dissipation processes, the charge pulses associated with the detection of identical x-rays are not necessarily equivalent in magnitude. Instead, they vary statistically about some mean value (see the aside on page 25). For a large number of pulses, the shape of the resulting distribution of values approximates a normal distribution. One indicator of the quality of a spectrometer is the width of this distribution relative to its height. This indicator is referred to as the spectral resolution and by convention is measured as the full width of the distribution at one-half its maximum height (FWHM). (It should be kept in mind that spectral resolution reflects the performance not only of the detector crystal but also of other components in the signal-processing chain.) Resolution is also a function of the energy of the x-ray measured. Therefore, resolution is conventionally specified for a given x-ray line and for given conditions of operation (typically the 5.9-keV manganese Kα line, at 1000 counts per second and an 8-μsec pulse processor time constant).

4.1.4 Detector Efficiency

Consideration must also be given to detector efficiency. After successfully escaping from the sample and reaching the x-ray detector, an x-ray may remain undetected for two important reasons. First, it may not reach the detector crystal itself. Because of the requirement for high-purity detectors, the crystal must be operated in a very clean, very high vacuum. In conventional EDS detectors, therefore, the crystal vacuum is maintained separately from the vacuum of the electron column. This isolation is achieved by enclosing the crystal within a tube, then sealing the end of the tube with a window of some material that is relatively transparent to the x-rays of interest. For many years, the preferred window material was beryllium.

Rolled to a thickness of 7.5 mm, beryllium withstands the pressure differential between crystal and sample environments and transmits x-rays from elements with atomic numbers 11 and greater. (X-rays with energies greater than 2 keV are transmitted by the beryllium window with nearly 100% efficiency.) X-rays lower in energy than 1keV are absorbed by the beryllium window and are therefore undetected.

In the late 1980's the first thin window that was capable of withstanding the pressure differential between the vacuum within the detector and the "atmosphere" in the vented sample chamber was introduced. Most detectors now use a polymer-based window supported on a silicon grid, which are transparent to x-rays down to 100eV which permits detection of beryllium while withstanding atmospheric pressure. These new materials can be tailored to enhance characteristics such as transmission or moisture resistance (see Figure 4-3.).

There are other barriers to x-rays as well—albeit less important ones than the detector window. X-rays may also be absorbed by contaminants on the window, by the conductive layer of metal on the surface of the detector crystal or by an inevitable dead layer of silicon just under the metal layer.

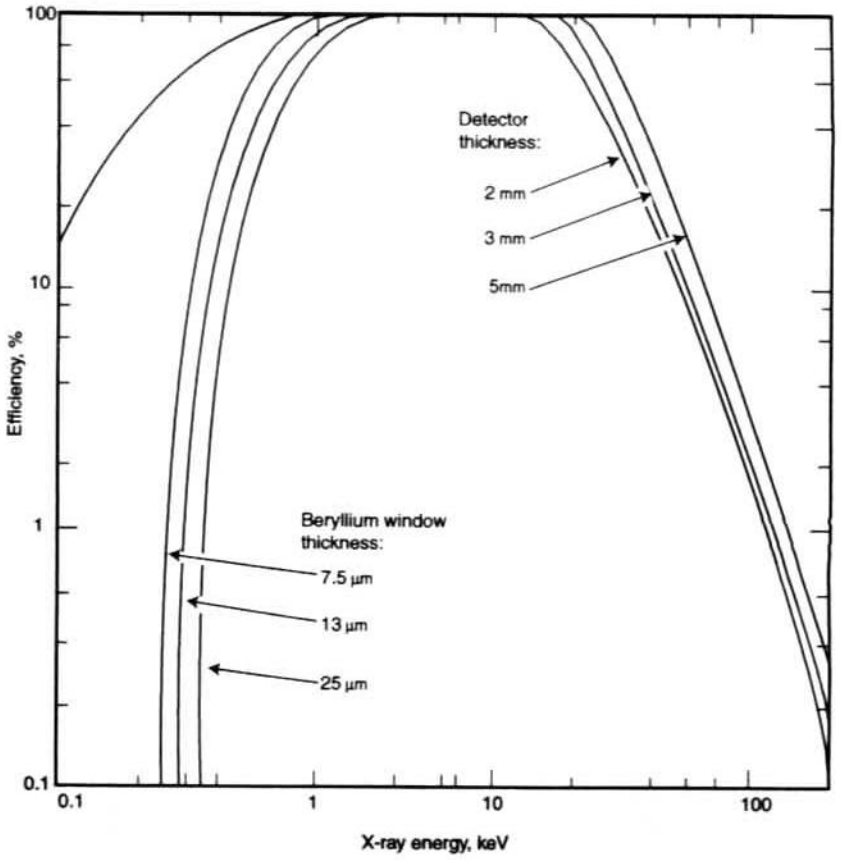

Figure 4-3. *Plot of theoretical detector efficiency as a function of x-ray energy. Curves are shown for three beryllium window thicknesses and three silicon detector thicknesses. The curve at the upper left is the theoretical efficiency of a windowless detector.*

Absorption within the window therefore limits the sensitivity of the x-ray detector to low-energy x-rays. A limit to the detection efficiency for high energy x-rays also exists. As x-rays increase in energy, there is an increasing probability that they will pass completely through the detector crystal, escaping with at least a fraction of their original energy. The thicker the crystal , the better it is at stopping high-energy x-rays. However, the detector-manufacturing process imposes a practical limit on crystal thickness so a thickness of 2 or 3 mm is typical. A 3-mm crystal maintains near 100% detection efficiency to almost 20 keV. Figure 4-3 also illustrates this effect of crystal thickness on detector efficiency.

4.1.5 The Dead Layer

The dead layer alluded to above is a layer at the silicon crystal surface it which neutralization has not been achieved in the lithium drifting process.

Excess holes therefore remain. The result is the phenomenon of incomplete charge collection, or charge trapping, in which charges created as a result of x-ray absorption may be trapped in the crystal rather than being swept out by the bias voltage to be measured in the charge pulse. The size of the detected charge pulse is therefore reduced by some amount, and the x-ray is assigned some energy lower than its true energy. These reduced energy measurements appear as a "tail" on the low-energy side of the detected peak. The ratio of the FWHM to the FWTM (full width at one-tenth maximum peak height) is sometimes used as an indication of how much low-energy tailing is present.

4.1.6 Escape Peaks

In addition to charge trapping, a second phenomenon sometimes occurs near the surface of the detector crystal. The ejection of a silicon photoelectron by the incoming x-ray is sometimes followed by the emission of an x-ray characteristic of silicon—the same deexcitation process that gave rise to the x-rays in the sample. If this x-ray is subsequently absorbed in the detector crystal, it contributes appropriately to the charge pulse measured for the original x- ray. However, should the silicon x-ray escape, carrying with it a well-defined amount of energy (1.74 keV, the energy of the silicon Kα x-ray), the energy measured for the detected x-ray will be less than the actual x-ray energy by exactly that amount. Therefore, as counts accumulate in an x-ray peak for any major constituent of the sample, an *escape peak* can be expected to appear at an energy 1.74 keV below that of the *parent peak*. This escape peak is simply the collection of counts from measurements that included escape events.

Escape peak intensities depend strongly on two parameters, the angle at which the original x-ray enters the detector crystal and the energy of the parent peak. The angle of x-ray incidence influences the average depth at which silicon x-rays are generated. Normal incidence tends to increase this average depth and thus reduce the number of escape events. At the other extreme, grazing incidence increases the number of escape events. Since it is governed by a curve like Figure 2-8, the likelihood of silicon ionization increases as the energy of the exciting x-rays approaches the silicon K-shell binding energy (1.84 keV) from above. Consequently, high-energy x-rays are likely to penetrate more deeply than low-energy x-rays before being absorbed. Escape events are thus most likely when the primary x-ray energy is just above 1.84 keV. No escape peaks are observed for parent peaks with energies less than 1.84 keV.

Although escape peaks will be present for all parent peaks above 1.84 keV, escape events are relatively rare under most conditions. Usually, the magnitude of an escape peak is, at most, a few percent of that of its parent peak.

4.2 Preamplifier

The next step in the signal-processing chain is the preamplifier. It is here that the current conducted by the detector crystal is integrated and amplified. An amplification circuit incorporating a field-effect transistor (FET) is the first stage. Early preamplifier designs incorporated resistive feedback at this stage; however, the electronic noise associated with this technique led to the development of alternative feedback mechanisms. Most commonly used today is a configuration referred to as pulsed optical feedback. In this design, the output of the FET is allowed to range between preestablished limits. Upon reaching the upper limit, a light-emitting diode (LED) shines on the FET and resets the circuit, capitalizing on the photoelectric response of the transistor.

The output of the amplification circuit, then, is a voltage sawtooth comprising slowly rising linear ramps (representing the detector and FET leakage current), upon which are superimposed step increases (see the signal emerging from the preamp in Figure 4-1). The magnitude of each step is proportional to the integrated current conducted by the detector for each x-ray event. In the interest of reducing thermal and transmission noise, the FET is positioned adjacent to the detector crystal and is cryogenically cooled.

At this point, it helps to introduce the concept of analyzer *deadtime*. To reiterate the analytical problem, the analyst is asked to derive from the number of x-rays measured the concentration of the emitting element. The most straightforward way of doing this is to compare the numbers of x-rays detected from two samples (namely, from the unknown and from a standard of known composition) under identical instrument operating conditions. Therefore, in the classical analysis scheme, the number of x-rays counted from an unknown is compared to the number of x-rays counted from a standard during a given period of excitation. There are certain times, however, during which the analyzer will not record a detected x-ray. During such times, it is said to be "dead." Therefore, two measurements made for equivalent real-time periods may be compared directly only if the amount of the deadtime during those periods is assumed to be the same.

Deadtime is introduced at several stages in the signal-processing chain. One source is the brief period during which the FET is reset by the pulsed optical feedback circuit. The deadtime arising from this source varies from one acquisition to another. For example, a sample that emits 1000 10-keV x-rays per second causes roughly twice as much current to flow through the FET circuit as one that emits 1000 5-keV x-rays per second. The FET circuit should therefore reset itself twice as often and exhibit twice the deadtime. Modern analyzers incorporate deadtime-correction circuitry that automatically accounts for such variations in deadtime. Spectral acquisition is then based upon live-time seconds rather than real-time seconds.

Other preamplifier designs do not cause reset deadtime. One such design is known as dynamic charge restoration. In this scheme, the circuit is essentially reset or restored as each pulse is processed.

4.3 Pulse Processor/Amplifier

The third step in the signal-processing chain is the pulse processor or main amplifier. At this point, the step increases generated by the preamplifier are conditioned for acceptance by an analog-to-digital converter. Two methods are in common use. The first involves an initial differentiation and subsequent multiple integrations of the step signal. The result is a roughly bell-shaped voltage pulse, the height of which corresponds to the magnitude of the step input. The multiple integrations can be thought of as filters designed to remove undesirable frequency components from the signal. The desired information is carried in the dc voltage changes associated with the step outputs of the preamplifier. Any short-duration (ac) variations in the signal level constitute noise. While converting the signal to a form acceptable for digitization, it is desirable to preserve the information contained in the step changes while attenuating or filtering out any noise.

Filters can be characterized by a parameter known as the time constant. The larger the time constant, the less sensitive the filter to high-frequency noise at the input. In the name of accuracy, then, it is desirable to operate at the largest possible time constant. However, the time constant is related to the length of time required for the output of the filter to reach a specified level, given an instantaneous change at the input, so it is also directly related to the time required to process each individual x-ray event. Thus, there is a trade-off between the *rate* at which x-rays can be processed (the count rate capability) and the *accuracy* with which each individual pulse can be processed (spectral resolution).

4.3.1 Time-Variant Processing

In the amplification method just described, the *time constant* remains the same for both the rising phase and the falling phase of each pulse. However, we can derive the information we need, namely, the height of the pulse, as soon as the pulse reaches its maximum intensity. The time during which the pulse is falling back to a zero level is essentially wasted. During this time, a subsequent pulse cannot be accepted, because it would be added to the level of the declining signal. A second method of pulse processing, known as time-variant processing, has therefore been developed to reduce this wasted time. In time-variant processing, a time constant is applied during the rising phase of the pulse that optimizes the information carried in the signal. Once the pulse maximum has been measured, the time constant is switched to a smaller value, allowing the pulse to fall off more rapidly. Time-variant processors offer a more attractive compromise between resolution and count rate, though current designs suffer some constraints in their use with electron column system. In particular, they are sensitive to variations in count rate, which unavoidably occur during the raster scan of an inhomogeneous sample.

4.3.2 Pulse Pileup Rejection

Each signal pulse must be measured individually with reference to a zero level and cannot be measured when superimposed upon either the leading edge or the trailing edge of a nearly coincident pulse (see Figure 4-4). *Pulse pileup rejection* is the technique by which nearly coincident pulses are rejected. All pileup rejection circuits depend upon the discrimination of the beginning of a pulse in a so-called fast-channel amplifier. Given knowledge of the time constants used in the processing amplifier, it is then possible to calculate when interfering overlaps have occurred. However, because of the requirement for fast-channel discrimination, pulse pileup rejection circuits lose their efficiency at low energies, where the amplitude of the x-ray events approaches that of noise events.

Pulse pileup rejection is another source of analyzer deadtime. In fact, because nearly coincident pulses must be rejected, an increase in the rate at which x-rays enter the detector does not necessarily result in an increase in the rate at which x-rays are accepted and processed. The higher the input rate, the greater the number of rejected pulses. As a rule of thumb, maximum throughput occurs when deadtime is about 60% of real time (Figure 4-5).

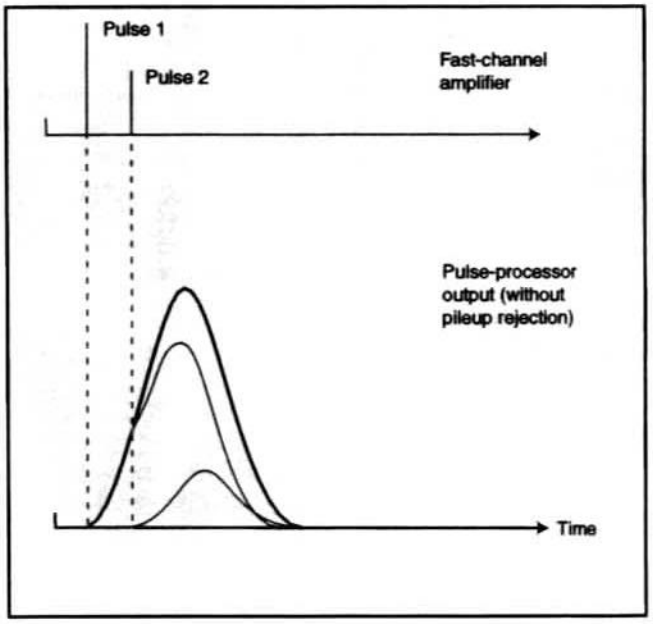

Figure 4-4. *Illustration of pileup. In the case shown here, failure to discriminate (and reject) the two pulses would lead to an anomalously large pulse being digitized and stored.*

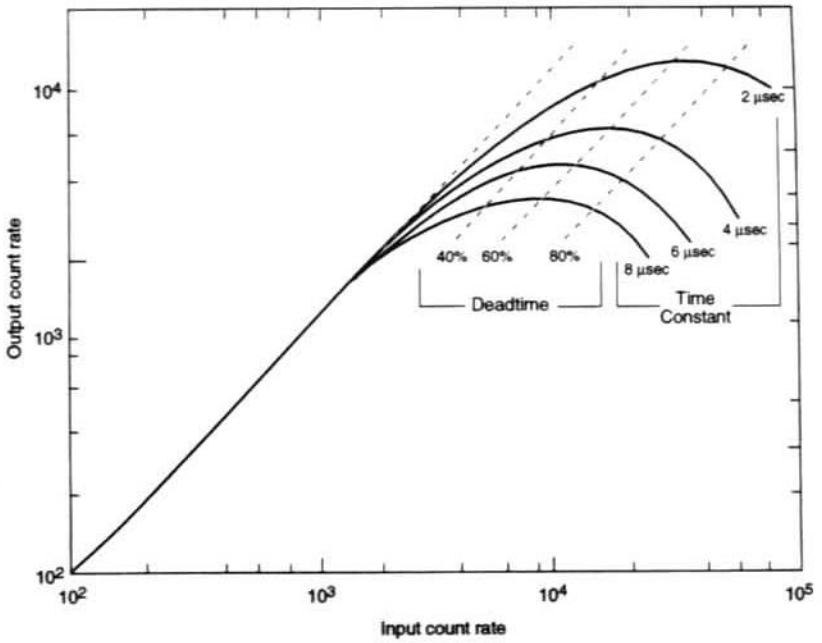

Figure 4-5. Plot of output count rate as a function of input count rate, for four pulse-shaping time constants. Because of the pulse pileup rejection circuitry, an input count rate that produces about 60% deadtime maximizes the output count rate for a given time constant.

4.4 EDC and Multichannel Analyzer

In the energy-to-digital converter, the height of the voltage pulse from the pulse processor (which is proportional to the energy of the detected x-ray) is measured and assigned a channel number. The number of counts in that channel of the multichannel analyzer is then increased by one. The most common energy-to-digital converter used in microanalysis systems is known as a timed capacitive discharge converter. In such a converter, the voltage pulse charges a capacitor, which is then allowed to discharge at a constant rate. The time required to discharge the capacitor is a measure of the height of the voltage pulse. The multichannel analyzer, then, is the means by which the signal information is accumulated and assembled into a spectrum. In addition, control of the display and the spectrometer is usually handled though a video terminal and keyboard associated with the multichannel analyzer.

Aside: Statistical Considerations

Deriving an energy distribution for x-rays emitted by a given sample depends ultimately on assigning an energy value to each detected x-ray. The errors implicit in making this assignment are of two types. The first we call *systematic error*, which includes instrumental errors (such as errors in calibration), errors in technique, errors due to environmental effects, and errors directly attributable to the analyst performing the measurements. To some extent, this type of error is controllable, and we shall assume that it is minimized. In any case, systematic error cannot generally be evaluated by any logical, mathematical means. The second type of error, *random error*, is not controllable; however, its magnitude can be estimated from theoretical considerations.

In light of these observations, this discussion deals with random error, that is, with events of an intrinsically random nature. The processes of x-ray emission and x-ray detection both involve such events. The result is that statistics enters any discussion of microanalysis at two

important points—in assigning an energy value to a spectral peak and in evaluating the intensity of that peak.

Normal Distribution and Standard Deviation

The breadth of each peak in an x-ray spectrum (for example, the one in Figure 1-3) indicates dearly that the energy of an individual x-ray cannot be measured exactly. The amount of charge the x-ray generates in the detector is vulnerable to random variations, and the electronic circuitry inevitably contributes noise to the signal. Consequently, a series of energy measurements of x-rays of energy E will form a distribution about a mean value, which we hope is very close to E.

This energy distribution can, for most practical purposes, be assumed to be an example of a *normal (or Gaussian) distribution* (Figure 4-6):

$$f(x) = \frac{1}{\sigma\sqrt{2\pi}} \exp\left[\frac{-(x-\bar{x})^2}{2\sigma^2}\right]$$

where $\bar{x}$ is the mean value (of energy in our case) and σ is the *standard deviation*. The standard deviation is an indicator of the breadth of the distribution. In a normal distribution with a standard deviation σ, 68.3% of all measurements of x fall between $\bar{x}$ - σ and $\bar{x}$ + σ, 95.4% fall between $\bar{x}$ - 2σ and $\bar{x}$ + 2σ, and 99.7% fall between $\bar{x}$ - 3$\sigma$and $\bar{x}$ + 3σ. One further fact is of particular interest. Note that the value $\bar{x}$ is itself a statistical parameter. If we make a series of evaluations of $\bar{x}$, each based on N measurements of x, the values of $\bar{x}$ will themselves form a normal distribution. This "distribution of averages" is characterized by the *standard deviation of the mean*, which, for N measurements of x, can be expressed as

$$\sigma_N = \frac{\sigma}{\sqrt{N}}$$

This gives us an idea of how close a single measured value of the mean ($\bar{x}$) is to the "true" value of E. If a spectral peak has a standard deviation of 100 eV and is the result of detecting 10,000 individual x-rays, we can take σ as 100 and N as 10,000. The resulting value of σ_n is 1 eV. This gives us considerable confidence that the mean of the measured peak is very close to the true energy of the electronic transition being observed.

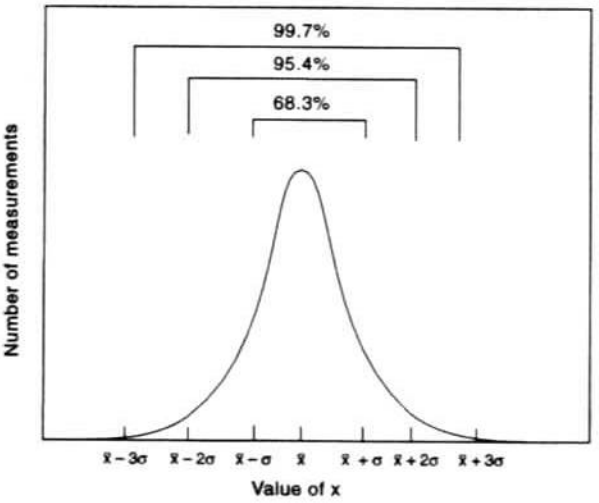

Figure 4-6. *The normal distribution function. The number of measurements that fall within one, two, and three standard deviations of the mean are 68.3%, 95.4%, and 99.7% of the total, respectively.*

Counting Error

In evaluating the intensity of a spectral peak, that is, the number of x-ray counts it comprises, we encounter a source of random error even more fundamental than those we have just mentioned. The emission and subsequent detection of a characteristic x-ray can, taken together, be regarded as a statistically independent event (unrelated to past or future events), which has a fixed probability of occurring within each infinitesimal time interval δt. Under conditions such as these, the number n of x-rays detected during any finite time interval is governed by the Poisson law:

$$P(n) = \frac{e^{-\bar{n}}\bar{n}^n}{n!}$$

where $P(n)$ is the probability of detecting exactly n x-rays and $\bar{n}$ is the mean number of x-rays counted during a large number of such trials. This equation says that, for a random process occurring at a constant average rate, we can, in a finite time interval, only estimate the true *average* rate. The confidence we have in the accuracy of our estimate can be no greater than that indicated by the breadth of the Poisson distribution—a plot of $P(n)$ versus n—and the inevitable error is called the *counting error*. The standard deviation of a Poisson distribution is

$$\sigma = \sqrt{\bar{n}}$$

and the *variance* (which we shall need later) is

$$\sigma^2 = \bar{n}$$

Furthermore, for fairly large values of $\bar{n}$, the Poisson distribution can be represented by an appropriate normal distribution. Accordingly, we can say that 68% of all measurements of n lie between $\bar{n} - \bar{n}^{1/2}$ and $\bar{n} + \bar{n}^{1/2}$ that 95% lie between $\bar{n} - 2\bar{n}^{1/2}$ and $\bar{n} + 2\bar{n}^{1/2}$

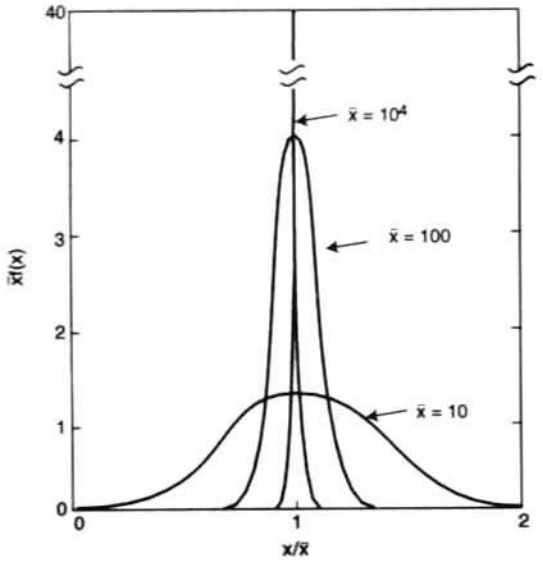

Figure 4-7. *Relative shapes for normal distributions with different means ($\bar{x}$) and with a $\sigma = x^{1/2}$. The abscissa is such that the width of each distribution is proportional to the relative precision; the ordinate is such that the integral of each is equal to unity.*

and so forth. Clearly, the larger the value of $\bar{n}$, the narrower the distribution relative to the mean (see Figure 4-7).This observation is reflected in the value of the *relative standard deviation*:

$$\varepsilon = \frac{\sigma}{\bar{x}}$$

or, for Poisson distributions only,

$$\varepsilon = \frac{\sqrt{\bar{n}}}{\bar{n}} = \frac{1}{\sqrt{\bar{n}}}$$

Relative error can also be expressed at higher *levels of confidence* by substituting 2σ or 3σ for σ in the equation for the relative standard deviation (see Figure 4-8).

What all this means is best shown in an example. Ignoring for a moment the problem of evaluating and removing background counts from the spectrum, let us assume that we have a spectral peak representing a single element. If that peak comprises 100 individual x-ray counts (and if we make the reasonable assumption that 100 is fairly close to $\bar{n}$), we can say, at a confidence level of 68%, that the relative counting error is no greater than

$$\varepsilon = \frac{1}{\sqrt{\bar{n}}} = \frac{1}{10} \quad \text{or } 10\%$$

The relative errors at 95% and 99% levels of confidence are 20% and 30%, respectively. If, on the other hand, our peak had contained 10,000 counts, the relative errors (at 68%, 95%, and 99% confidence levels) would be 1%, 2%, and 3%, respectively.

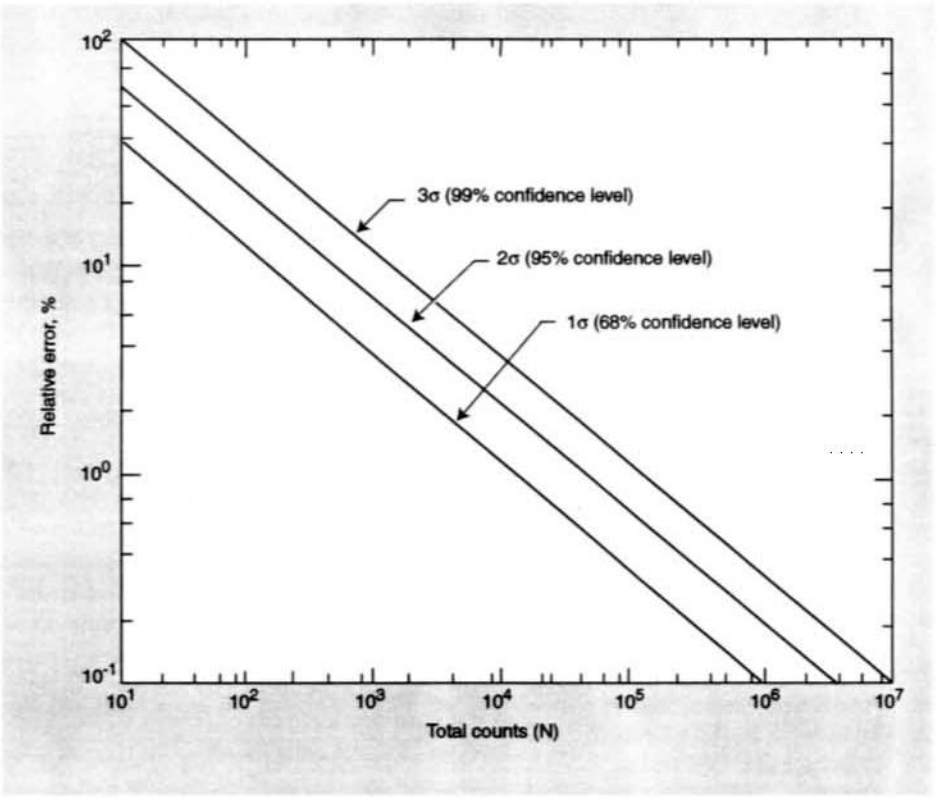

Figure 4-8. *Plot of relative error as a function of total counts for three levels of confidence.*

Finally, it must be borne in mind that the counting error is only a lower limit on the errors involved in quantitative estimates of element concentration based on peak intensities.

Minimum Detection Limits

We encounter another important statistical consideration in trace analyses, where instrumental capability is being strained in merely determining whether an element is present or not. In fact, at sufficiently low concentrations, one can only conclude that "if element X is present at all, its concentration must be less than ..." This limit is the *minimum detection limit (MDL)*.

In microanalysis we are concerned with measuring the net peak intensity, that is, the intensity of the characteristic x-ray signal above the background signal. As we mentioned above, there is counting error in any measurement of peak intensity. Likewise, the background signal itself is susceptible to counting error. Therefore, the microanalyst is confronted with the problem of distinguishing between random fluctuations in the background and real peaks. Furthermore, the microanalyst must establish a confidence level to be maintained in any assertion that an element is present at the MDL. For example, a 95% confidence level would be consistent with the statement that, in a large number of observations, 95% of the observations indicating the presence of an element at the MDL reflect the actual presence of that element, whereas 5% of such observations reflect only random fluctuations in background count rate. Ninety-five percent is a typical confidence level. Conveniently, 95% confidence may be obtained if the criterion for peak presence is set as a "fluctuation" greater than two standard deviations above the expected average intensity.

The extent of the random background fluctuations can be derived from the Poisson law discussed above. If a region of interest is established, we can therefore assess the probability that the number of background counts in that region will differ from the mean by some

specified amount. And again, the magnitude of the random fluctuations is a function of the total number of counts in the region of interest; specifically, the standard deviation for the background counts is

$$\sigma_b = \sqrt{\bar{n}_b}$$

where the subscript *b* indicates that we are now talking about the background.

In practice, MDLs are influenced by a number of experimental factors including instrument stability, spectral peak overlaps, and interactions within the sample matrix. However, in an ideal case—that of an unobstructed peal on a smoothly varying background—a theoretical MDL can be established. First, we need to know that the variance of the sum of, or the difference between, two values taken from statistically independent distributions is equal to the sum of the variances of the two distributions. Thus, for net counts,

$$\sigma^2_{net} = \sigma^2_b + \sigma^2_{total} = \bar{n}_b + (\bar{n}_b + \bar{n}_{net}) = 2\bar{n}_b + \bar{n}_{net}$$

where the subscript total refers to the total counts in a region of interest. This must be so, because the number of net counts is computed as the difference between the total number of counts and the estimated number of background counts. Now we can ask, "How many net counts must we detect to be sure (or 95% sure) that we are not merely seeing a statistical fluctuation in that background?" The answer is that the number of net counts must exceed twice the standard deviation of net counts. (Otherwise, there is at least a 5% chance that the "net counts" we observe arise merely from statistical fluctuations in the total counts and the estimated background counts.) This requires that

$$\begin{aligned} n_{net} &\geq 2\sigma_{net} \\ &\geq 2\sqrt{2\bar{n}_b + \bar{n}_{net}} \end{aligned}$$

or, assuming that measured counts (*n*) are close to the respective means (n) and that, for small net peaks, $n_b \gg n_{net}$,

$$n_{net} \geq 2\sqrt{2\bar{n}_b} \cong 3\sqrt{\bar{n}_b}$$

where, once again, n_{net} is the number of computed net counts and n_b is the number of computed background counts. The MDL is the concentration corresponding to n_{net}. Since the MDL is a function of counts, it is also a function of counting time. The size of the net peak increases linearly with acquisition time and must eventually exceed $3n_b^{1/2}$ (which increases more slowly), whatever the concentration of the element in question. Obviously, however, there is a practical limit to increasing the acquisition time as a means for lowering the MDL. Nonetheless, MDLs as low as 0.01% are feasible under certain conditions. Furthermore, the microanalytical aspect of the electron probe device yields a detection limit in terms of absolute amounts (the *mass limit*) that is very low—under the best analytical conditions, as low as 10^{-15} to10^{-16} grams. More extensive treatments of MDLs are available in References 5 and 6.